# Receiver Concepts and Resource Allocation for OSC Downlink Transmission*

Michael A. Ruder[1], Raimund Meyer[2], Frank Obernosterer[2], Hans Kalveram[2], Robert Schober[1,2], and Wolfgang H. Gerstacker[1,2]
[1]Institute for Digital Communications, Universität Erlangen-Nürnberg,
Cauerstraße 7, D-91058 Erlangen, Germany, {ruder, schober, gersta}@LNT.de
[2]Com-Research GmbH, Wiesengrundstr. 4, D-90765 Fürth, Germany, {raimund.meyer, frank.obernosterer, hans.kalveram}@com-research.de



***Abstract*—Voice services over Adaptive Multi-user channels on One Slot (VAMOS) has been standardized as an extension to the Global System for Mobile Communications (GSM). The aim of VAMOS is to increase the capacity of GSM, while maintaining backward compatibility with the legacy system. To this end, the Orthogonal Sub-channels (OSC) concept is employed, where two Gaussian minimum-shift keying (GMSK) signals are transmitted in the same time slot and with the same carrier frequency. To fully exploit the possible capacity gain of OSC, new receiver concepts are necessary. In contrast to the base station, where multiple antennas can be employed, the mobile station is typically equipped with only one receive antenna. Therefore, the downlink receiver design is a very challenging task. Different concepts for channel estimation, user separation, and equalization at the receiver of an OSC downlink transmission are introduced in this paper. Furthermore, the system capacity must be improved by suitable downlink power and resource allocation algorithms. Making realistic assumptions on the information available at the base station, an algorithm for joint power and radio resource allocation is proposed. Simulation results show the excellent performance of the proposed channel estimation algorithms, equalization schemes, and joint radio resource and power allocation algorithms in realistic VAMOS environments.**

## I. Introduction

The Global System for Mobile Communications (GSM) is still by far the most popular cellular communication system worldwide. Especially in emerging markets, there is the need for a major voice capacity enhancement of GSM in order to meet the demands of the customers. Different approaches to improve the spectral efficiency of GSM have been discussed. For example, a tighter frequency reuse might be employed which, however, leads to increased interference from other users within the system. Interference suppression techniques are required in order to avoid a performance degradation for small frequency reuse factors. To this end, single antenna interference cancellation (SAIC) algorithms have been developed, e.g. [1], [2], exploiting the special properties of the Gaussian minimum-shift keying (GMSK) modulation used in GSM, which can be well approximated by filtered binary phase-shift keying (BPSK). These algorithms are already employed in commercial GSM terminals. Especially for downlink transmission they are highly beneficial because only a single receive antenna is required for interference suppression.

With the study item Multi-User Reusing One Slot (MUROS) in 3GPP TSG GERAN an alternative to smaller reuse factors was proposed for voice capacity enhancement, cf. [3], [4]. The MUROS study item led to the standardization of Voice services over Adaptive Multi-user channels on One Slot (VAMOS) [5], where the capacity is increased by deliberately overlaying two users in the same time slot and frequency resource within a cell. By this, in principle, the capacity can be doubled. Therefore, VAMOS is also one of the key enablers for the refarming of spectrum [6]. However, in the downlink, only a single receive antenna can be assumed for both involved mobile stations (MSs), and for each of the MSs, the two overlaid transmit signals of the base station (BS) travel through the same propagation channel. With the aim of enabling a sufficiently good user separation and backward compatibility to the legacy GSM system, the Orthogonal Sub-channels (OSC) concept is applied in the downlink of VAMOS [7]. In order to take into account that each user in a VAMOS user pair may experience different propagation conditions (large-scale fading), different powers are assigned to both transmit signals resulting in a certain subchannel power imbalance ratio (SCPIR) [3].

Efficient receiver algorithms are necessary to cope with the interference in a VAMOS OSC downlink system. In the downlink, joint estimation of the SCPIR and the channel impulse response can be accomplished with only a small estimation performance loss compared to non-OSC GSM transmission [8]. In the literature, few papers consider VAMOS downlink receiver algorithms. In [9], SAIC receiver algorithms for VAMOS downlink transmission are proposed. However, these algorithms are only optimized to suppress GMSK interferers. The algorithms proposed in this paper have an improved capability to also mitigate OSC interferers.

Since the interference situation is crucial for the overall user experience, the performance of the receiver algorithms has to be evaluated in a network scenario. Radio resource allocation (RRA) is considered here for the VAMOS downlink, which is more challenging than RRA for the uplink, where a standard multiple-input multiple-output (MIMO) transmission scenario arises. So far, only a very limited number of results on RRA for OSC and VAMOS are available. In [10], RRA for the VAMOS up- and downlink is studied. However, [10] does not consider the problem of unknown interference caused

* This paper has been presented in part at the IEEE International Symposium on Personal, Indoor and Mobile Radio Communications (PIMRC) 2009 and 2011, and the IEEE International Conference on Communications in China (ICCC) 2012.

by frequency hopping (FH) and random speech activity. It is assumed in [10] that the interference level is known and the interference consists of only one dominant out-of-cell GMSK interferer. In [11], we have proposed an RRA algorithm that takes into account unknown interference. In the system model considered in [11], the interference is caused by GMSK as well as OSC co-channel interferers. Although the BS assigns users to VAMOS pairs and determines the frequencies and the transmit powers for the downlink, it is not possible to estimate the interference level for each user and in each burst due to FH. The task of the proposed RRA algorithm is to minimize the required transmit power of the BS, while trying to achieve some target frame error rate (FER) at each MS. The algorithm in [11] is presented in more detail in this paper. Additionally the influence of discontinuous transmission (DTX), where no signal is transmitted during speech pauses, is analyzed, and a hot spot scenario is investigated.

In summary, this paper makes the following major novel contributions:

- The link and network aspects of downlink OSC transmission are presented for a common system model.
- A novel enhanced V-MIC receiver, requiring only one receive antenna, is derived. The superior FER performance compared to the receivers in [12] is confirmed by link level simulation results.
- Various receiver algorithms are evaluated in network level simulations including RRA. The beneficial influence of advanced receiver algorithms on the network capacity is studied, where the novel V-MIC exhibits significant capacity gains.
- Discontinuous transmission and a hot spot scenario, where only no-VAMOS interference is present, are analyzed in network level simulations. The capacity gain enabled by OSC downlink transmission in these scenarios is quantified by simulation results.

The paper is organized as follows. Section II introduces the system model of a VAMOS downlink transmission. In Section III, channel estimation for the OSC downlink is discussed, and Section IV provides different equalization concepts and outlines the link-to-system mapping used for faster performance evaluation of the transmission system. A joint radio resource and power allocation algorithm is presented in Section V. Sections VI and VII provide simulation results and conclusions, respectively.

*Notation:* $\mathcal{E}\{\cdot\}$, $(\cdot)^T$, $(\cdot)^*$, and $(\cdot)^H$ denote expectation, transposition, conjugation, and Hermitian transposition, respectively. $\ln(x)$ denotes the natural logarithm of $x$. Bold lower case letters and bold upper case letters refer to column vectors and matrices, respectively. $\mathbf{I}_X$ denotes the $X \times X$ identity matrix. $\mathrm{Im}\{\cdot\}$ and $\mathrm{Re}\{\cdot\}$ stand for the imaginary and real parts of a complex number, respectively. $[\mathbf{A}]_{m,n}$ is the element in the $m$th row and $n$th column of matrix $\mathbf{A}$. $\mathcal{Z}^{-1}\{\cdot\}$ denotes the inverse $z$-transform. $< \cdot, \cdot >$ and $(\cdot) * (\cdot)$ stand for the inner product of two vectors and the convolution operation, respectively. $\lfloor x \rfloor$ denotes the largest integer not greater than $x$. We use $f(x) = O(g(x))$ if and only if there exists a positive real number $C$ and a real number $x_0$ such that $|f(x)| \leq C \cdot |g(x)| \; \forall \; x > x_0$.

## II. System Model

In the considered model of an OSC downlink transmission, we focus on one specific cell. The BS of this cell serves a random number $N$ of users $i \in \mathcal{U} = \{1,\ 2,\ \ldots,\ N\}$. Up to two user signals, corresponding to one pair, transmit in the same time slot and the same frequency resource. According to the OSC concept [3], the first user of the pair (user $o \in \mathcal{U}$) and the second user (user $p \in \mathcal{U}$, $o \neq p$) have a phase difference of $90°$. In the equivalent complex baseband, the received signal at MS $o$ after GMSK derotation can be written as

$$\tilde{r}_o[k] = \sqrt{G_o} \sum_{\kappa=0}^{q_h} \tilde{h}_o[\kappa] \left( \sqrt{P_o} a_o[k-\kappa] + j\sqrt{P_p} a_p[k-\kappa] \right) + \tilde{n}_o[k] + \tilde{q}_o[k]. \quad (1)$$

Here, the discrete-time channel impulse response (CIR) $\tilde{h}_o[k]$ of order $q_h$ is normalized to unit energy without loss of generality and comprises the effects of GMSK modulation, the mobile channel from the BS to the considered user $o$, receiver input filtering, and GMSK derotation at the receiver. The path gain for transmission from the BS to the receiver of user $o$ is denoted by $G_o$. It comprises the distance attenuation and the large-scale fading, whereas $\tilde{h}_o[k]$ only characterizes the small-scale fading for user $o$. We assume that $\tilde{h}_o[k]$ is constant for the duration of one burst (block fading model) and unknown to the BS for RRA. $G_o$ changes only very slowly and is therefore assumed to be constant and known to the BS with sufficient accuracy by feedback from the MS. Interleaving is applied over one frame, which comprises $N_{\mathrm{bursts}}$ bursts. $a_o[k]$ and $a_p[k]$ refer to the BPSK transmit symbols of users $o$ and $p$, respectively, and both symbols have variance $\sigma_a^2$. The average transmit powers for users $o$ and $p$ are denoted by $P_o$ and $P_p$, respectively. $\tilde{n}_o[k]$ and $\tilde{q}_o[k]$ refer to discrete-time additive white Gaussian noise (AWGN) of variance $\sigma_{\tilde{n}}^2$ and adjacent plus co-channel interference from other cells at the receiver of user $o$, respectively. The received signal $\tilde{r}_o[k]$ according to (1) is normalized by multiplication with $1/\sqrt{P_o}$ resulting in

$$r_o[k] = \sum_{\kappa=0}^{q_h} h_o[\kappa] \left( a_o[k-\kappa] + j\, b\, a_p[k-\kappa] \right) + n_o[k] + q_o[k]. \quad (2)$$

Here, the overall CIR of user $o$ is denoted by $h_o[\kappa] = \sqrt{G_o}\, \tilde{h}_o[\kappa]$, where the CIR of user $p$ is the CIR of user $o$ multiplied by $j$ and scaled by a factor $b = \sqrt{P_p}/\sqrt{P_o}$, which is unknown at the receiver. $n_o[k]$ refers to AWGN with variance $\sigma_{n_o}^2$. The variance of the interference $q_o[k]$ is denoted by $\sigma_{q_o}^2$, assumed to be constant within each burst due to synchronized network operation, and different for each MS. The received signal for user $p$ can be obtained analogously after exchanging $o$ and $p$ in (2) and redefining $h_o[\kappa]$. Single user GMSK transmission for user $o$ is included in (1) as a special case with $P_p = 0$ and in (2) with $b = 0$. The average signal-to-noise ratio (SNR) of user $o$ is given by

$$\mathrm{SNR}_o = (G_o P_o \sigma_a^2)/\sigma_{\tilde{n}}^2. \quad (3)$$

Due to the fact that the power for each user within a pair can be allocated individually, a power imbalance between the users arises. The corresponding SCPIR for user $o$ is defined

as

$$\mathrm{SCPIR}_o = 10\log_{10}(P_o/P_p) = 10\log_{10}(1/b^2). \quad (4)$$

$\mathrm{SCPIR}_o$ specifies the difference of both transmit powers within one pair in dB. Obviously, $\mathrm{SCPIR}_p = -\mathrm{SCPIR}_o$ is valid. Due to receiver constraints, the power imbalance within one pair is limited to a maximum value [13]. The maximal allowed absolute value of SCPIR for RRA is denoted by $\mathrm{SCPIR}_{\max}$, i.e., $|\mathrm{SCPIR}_i| \leq \mathrm{SCPIR}_{\max}$ must be valid for any user $i$.

## III. Channel Estimation

As an initial task, we need to obtain estimates of the CIR and the SCPIR for the subsequent detection algorithms. It should be taken into account that both user signals propagate to user $o$ through the same channel. We can rewrite (2) in matrix-vector notation as

$$\mathbf{r}_o = \mathbf{A}_o\,\mathbf{h}_o + b\,\mathbf{A}_p\,\mathbf{h}_o + \mathbf{n}_o + \mathbf{q}_o, \quad (5)$$

where $\mathbf{r}_o$ denotes the vector of the normalized received symbols corresponding to the time-aligned training sequences of both users, $\mathbf{A}_o$ and $\mathbf{A}_p$ represent $(N_{\mathrm{tr}}-q_h)\times(q_h+1)$ Toeplitz convolution matrices corresponding to the training sequences of users $o$ and $p$, respectively, with training sequence length $N_{\mathrm{tr}}$, and $\mathbf{h}_o = [h_o[0]\,h_o[1]\,\ldots\,h_o[q_h]]^T$. $\mathbf{n}_o$ and $\mathbf{q}_o$ are vectors containing the noise and interference contributions, respectively. For simplicity, factor $j$ in (2) has been absorbed in $\mathbf{A}_p$. Furthermore, for channel estimation it is assumed that the composite impairment $\mathbf{w}_o = \mathbf{n}_o + \mathbf{q}_o$ is a Gaussian vector with statistically independent entries having variance $\sigma^2_{w_o}$.

### A. Joint ML Estimation of $\mathbf{h}_o$ and $b$

The joint maximum-likelihood (ML) estimates for $\mathbf{h}_o$ and $b$ are obtained by minimizing the $L_2$-norm of the error vector $\mathbf{e} = \mathbf{r}_o - \mathbf{A}_o\,\hat{\mathbf{h}}_o - \hat{b}\,\mathbf{A}_p\,\hat{\mathbf{h}}_o$, where $\hat{\mathbf{h}}_o$ and $\hat{b}$ denote the estimated quantities. Differentiating $\mathbf{e}^H\,\mathbf{e}$ with respect to $\hat{\mathbf{h}}_o^*$ and $\hat{b}$ and setting the derivatives to zero results in the following two conditions for the ML estimates of $\mathbf{h}_o$ and $b$:

$$\hat{\mathbf{h}}_o = \left(\left(\mathbf{A}_o^H + \hat{b}\,\mathbf{A}_p^H\right)\left(\mathbf{A}_o + \hat{b}\,\mathbf{A}_p\right)\right)^{-1}\left(\mathbf{A}_o^H + \hat{b}\,\mathbf{A}_p^H\right)\mathbf{r}_o \quad (6)$$

and

$$\hat{b} = \frac{1}{2}\left(\hat{\mathbf{h}}_o^H\,\mathbf{A}_p^H\,\mathbf{A}_p\,\hat{\mathbf{h}}_o\right)^{-1}\left(\left(\hat{\mathbf{h}}_o^H\,\mathbf{A}_p^H\right)\left(\mathbf{r}_o - \mathbf{A}_o\,\hat{\mathbf{h}}_o\right) + \left(\mathbf{r}_o^H - \hat{\mathbf{h}}_o^H\,\mathbf{A}_o^H\right)\left(\mathbf{A}_p\,\hat{\mathbf{h}}_o\right)\right). \quad (7)$$

Eqs. (6) and (7) may be also viewed as the ML channel estimate for a given $b$ and the ML estimate of $b$ for a given channel vector, respectively [14]. However, it does not seem possible to obtain a closed-form solution for $\hat{\mathbf{h}}_o$ and $\hat{b}$ from the two coupled equations. Thus, a solution might be calculated iteratively by inserting an initial choice for $\hat{b}$ in (6), using the resulting channel vector for refining $\hat{b}$ via (7), and so on, until convergence is reached.

### B. Blind Estimation of $b$

In an alternative approach, $b$ is first estimated from the received vector according to an ML criterion, assuming only knowledge of the channel statistics and both training sequences. Subsequently, the ML channel estimation is performed with the obtained $\hat{b}$ using (6).

Assuming $\mathbf{h}_o$ is a complex Gaussian vector with autocorrelation matrix $\mathbf{\Phi}_{h_o h_o} = \mathcal{E}\{\mathbf{h}_o\,\mathbf{h}_o^H\}$, the probability density function (pdf) of the received vector conditioned on $b$ may be expressed as

$$\mathrm{pdf}(\mathbf{r}_o\,|\,b) = \frac{1}{\pi^M\,\det\left(\mathbf{\Phi}_{r_o r_o|b}\right)}\exp\left(-\mathbf{r}_o^H\,\mathbf{\Phi}^{-1}_{r_o r_o|b}\,\mathbf{r}_o\right), \quad (8)$$

where $M = N_{\mathrm{tr}} - q_h$ and $\mathbf{\Phi}_{r_o r_o|b} = \mathcal{E}\left\{\mathbf{r}_o\,\mathbf{r}_o^H\,|\,b\right\}$,

$$\mathbf{\Phi}_{r_o r_o|b} = \left(\mathbf{A}_o + b\,\mathbf{A}_p\right)\,\mathbf{\Phi}_{h_o h_o}\left(\mathbf{A}_o + b\,\mathbf{A}_p\right)^H + \sigma^2_{w_o}\,\mathbf{I}_M. \quad (9)$$

The ML estimate for $b$ can be obtained by maximizing $\ln\left(\mathrm{pdf}(\mathbf{r}_o\,|\,b)\right)$ using (8) and (9):

$$\begin{aligned}\hat{b} &= \underset{\tilde{b}}{\mathrm{argmax}}\left\{-\mathbf{r}_o^H\,\mathbf{\Phi}^{-1}_{r_o r_o\,|\,\tilde{b}}\,\mathbf{r}_o - \ln\left[\det\left(\mathbf{\Phi}_{r_o r_o\,|\,\tilde{b}}\right)\right]\right\}\\ &= \underset{\tilde{b}}{\mathrm{argmin}}\left\{\mathbf{r}_o^H\left[\left(\mathbf{A}_o + \tilde{b}\,\mathbf{A}_p\right)\mathbf{\Phi}_{h_o h_o}\left(\mathbf{A}_o + \tilde{b}\,\mathbf{A}_p\right)^H + \sigma^2_{w_o}\,\mathbf{I}_M\right]^{-1}\mathbf{r}_o + \ln\left[\det\left(\left(\mathbf{A}_o + \tilde{b}\,\mathbf{A}_p\right)\mathbf{\Phi}_{h_o h_o}\right.\right.\right.\\ &\quad\left.\left.\left.\times\left(\mathbf{A}_o + \tilde{b}\,\mathbf{A}_p\right)^H + \sigma^2_{w_o}\,\mathbf{I}_M\right)\right]\right\}. \quad (10)\end{aligned}$$

Minimization of the one-dimensional function in (10) might be performed by a Golden section search technique [15].

It is interesting to compare the computational complexity of the algorithms described in Section III-A and III-B. If we assume the joint ML estimation in Section III-A needs $N_{\mathrm{it}}$ computations of (6) and (7) to reach convergence, the computational complexity in terms of complex multiplications is dominated by the matrix multiplication in Eq. (6) and can be approximated as $O(N_{\mathrm{it}}\cdot(q_h+1)^2(N_{\mathrm{tr}}-q_h))$. On the other hand, for the algorithm in Section III-B, the dominant terms are the inversion and determinant operations. If we assume that also $N_{\mathrm{it}}$ iterations are necessary for the minimization of (10), the computational complexity of the blind estimation algorithm can be approximated as $O(N_{\mathrm{it}}\cdot(N_{\mathrm{tr}}-q_h)^3)$. Thus, we conclude that the computational complexity of the joint ML estimation is lower than that of the blind estimation of $b$. Simulations have shown that, in principle, both proposed estimation approaches for $b$ perform equally well under practical conditions.

## IV. Equalization and Interference Cancellation

In the following, different equalization and interference cancellation algorithms are introduced.

### A. Joint Maximum-Likelihood Sequence Estimation (MLSE)

In noise limited scenarios, joint maximum-likelihood sequence estimation (MLSE) of sequences $a_o[\cdot]$ and $a_p[\cdot]$ (or a corresponding soft-output Viterbi algorithm [16] or Bahl–Cocke–Jelinek–Raviv (BCJR) algorithm [17] producing soft

outputs) is optimum. For this, a Viterbi algorithm (VA) in a trellis diagram with states

$$\tilde{\boldsymbol{S}}[k] = [\tilde{a}_o[k-1]\,\tilde{a}_p[k-1]\,\ldots\,\tilde{a}_o[k-q_h]\,\tilde{a}_p[k-q_h]], \quad (11)$$

where $\tilde{a}_o[\cdot]$, $\tilde{a}_p[\cdot]$ denote the trial symbols of the sequence estimator, can be used. The branch metric for the state transitions is given by

$$\lambda[k] = \left| r_o[k] - \sum_{\kappa=0}^{q_h} \hat{h}_o[\kappa]\,\tilde{a}_o[k-\kappa] - j\,\hat{b}\,\sum_{\kappa=0}^{q_h} \hat{h}_o[\kappa]\,\tilde{a}_p[k-\kappa] \right|^2. \quad (12)$$

Equivalently, an MLSE for the modified 4QAM constellation $\{-1-j\,\hat{b},\,-1+j\,\hat{b},\,+1-j\,\hat{b},\,+1+j\,\hat{b}\}$ can be applied. In both cases, the VA requires $4^{q_h}$ states.

### *B. Mono Interference Cancellation (MIC)*

For reconstruction of the sequence of interest $a_o[\cdot]$, also a standard SAIC algorithm can be employed. Therefore, legacy MSs supporting Downlink Advanced Receiver Performance (DARP) phase I [18] can be used also for VAMOS without any change if legacy training sequences are employed. By a simple pure software update, also the eight new VAMOS training sequences [3] can be taken into account in a straightforward manner in an MS with SAIC receiver. Thus, in the following, the MIC algorithm from [1], [19], [20] is briefly reviewed in the context of VAMOS.

An arbitrary non-zero complex number $c$ is selected and a corresponding number $c^{\perp} = \mathrm{Im}\{c\} - j\,\mathrm{Re}\{c\}$ is generated. $c$ and $c^{\perp}$ may be interpreted as mutually orthogonal two-dimensional vectors. The received signal is first filtered with a complex-valued filter with coefficients $f[\kappa]$ and then projected onto $c$, i.e., the real-valued signal

$$y_o[k] = \mathcal{P}_c\Big\{ \sum_{\kappa=0}^{q_f} f[\kappa]\,r_o[k-\kappa] \Big\} \quad (13)$$

is formed, where $\mathcal{P}_c\{x\}$ denotes the coefficient of projection of a complex number $x$ onto $c$,

$$\mathcal{P}_c\{x\} = \frac{<x,\,c>}{|c|^2} = \frac{\mathrm{Re}\{x\,c^*\}}{|c|^2}. \quad (14)$$

It is shown in [1], that the filter impulse response $f[\kappa]$ can be chosen for perfect elimination of signal contributions originating from $a_p[\cdot]$ (assuming $a_o[\cdot]$ is the desired sequence) if the filter order $q_f$ is sufficiently high. After filtering and projection, $a_o[\cdot]$ can be reconstructed by trellis-based equalization. An adaptive implementation of the MIC algorithm is also described in [1] which requires only knowledge of the training sequence of the desired user but no explicit channel knowledge.

In typical urban (TU) environments, channel snapshots where a single tap dominates arise frequently. Therefore, we consider the case $h_o[0] \neq 0$, $h_o[\kappa] = 0$, $\kappa \neq 0$ ($q_h = 0$). The single effective channel tap $j\,b\,h_o[0]$ of the second user is rotated by 90° compared to that of the first user. Therefore, in this case, orthogonal subchannels result also at the receiver side. According to [1], suppression of the second user is possible without any loss in SNR, and $\mathrm{SNR} = 2\,|h_o[0]|^2\,\sigma_a^2/\sigma_{n_o}^2$ is valid after MIC if interference from other cells is absent ($q_o[k] = 0$). However, both subchannel contributions are not orthogonal anymore at the receiver side for $q_h > 0$, and in general an SNR loss due to filtering and projection cannot be avoided. Hence, as long as interference from other cells is absent, joint MLSE performs better than MIC which may be viewed as a suboptimum equalizer for QPSK-type signals in this case.

It should be noted that MIC is beneficial also for scenarios with several interferers [1]. Here, the minimum mean-squared error (MMSE) filter found by adaptation is a kind of compromise solution adjusted to the interference mixture. Given this and the fact that the interference created by the other VAMOS pair user of the same BS is close to orthogonal to the desired user signal in many cases for TU scenarios, it is expected that MIC performs better than joint MLSE in scenarios with additional interference from other cells.

### *C. MIC Receiver with Successive Interference Cancellation*

Because joint MLSE degrades significantly if external interference is present and DARP phase I receivers, such as a receiver employing the MIC algorithm [1], typically exhibit a good performance only if the signal of the second VAMOS user is not much stronger than that of the considered user, more sophisticated schemes are of interest for interference limited scenarios. For this purpose, we exploit the fact that in contrast to the standard SAIC problem, the training sequences corresponding to $a_o[k]$ *and* $a_p[k]$ are known at the MS, and both signals are time aligned. Therefore, in principle, it is possible to reconstruct $a_o[\cdot]$ and $a_p[\cdot]$ in the same MS using two separate MIC algorithms.

In a MIC receiver with successive interference cancellation (SIC), channel estimation according to Section III is performed first. If $\hat{b} \geq b_0$ (e.g. $b_0 = 1.0$), $a_p[\cdot]$ is reconstructed first by combining the MIC algorithm with a subsequent trellis-based equalization yielding estimates $\hat{a}_p[\cdot]$. In the next step, the contribution of $a_p[\cdot]$ is canceled from the received signal, resulting in a signal

$$r_{c,o}[k] = r_o[k] - j\,\hat{b}\,\sum_{\kappa=0}^{q_h} \hat{h}_o[\kappa]\,\hat{a}_p[k-\kappa], \quad (15)$$

which is fed into another MIC and equalization stage in order to reconstruct $a_o[\cdot]$. Because $r_{c,o}[k]$ contains no (or considerably reduced) contributions from $a_p[\cdot]$, interference from other cells can be much better combated now by the second MIC.

If $\hat{b} < b_0$, only a standard MIC is employed for reconstruction of $a_o[\cdot]$ because successive interference cancellation most likely would suffer from error propagation.

In a typical implementation, the complexity of MIC with SIC is about 2.5 times higher than that of the standard MIC, which is considered affordable in a typical modern MS.

### *D. Enhanced VAMOS-MIC (V-MIC)*

To further enhance the performance of the SIC receiver and to avoid the switching between different receiver types depending on $\hat{b}$, an algorithm called VAMOS mono interference cancellation (V-MIC) can be used. The performance of

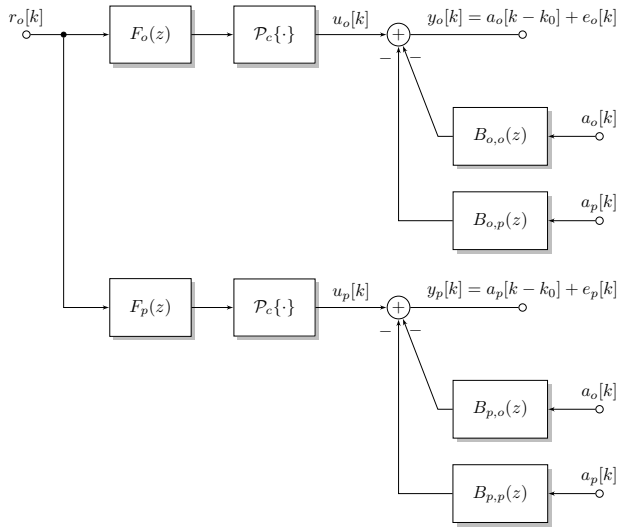


Fig. 1. V-MIC structure for filter adaptation.

this scheme was first reported in [21]. In the following, a detailed description of the algorithm is provided. The basic idea of this enhanced receiver is to filter the received signal twice in parallel. In both filtering operations, only out-of-cell interference is suppressed, while the intersymbol interference and interuser interference within the VAMOS pair are left in the signal. Both prefiltered signals, representing the signals of users $o$ and $p$, are then fed to a joint MLSE. A similar idea has also been presented in [22] for the uplink, but the algorithm in [22] relies on multiple receive antennas. The V-MIC presented in the following requires only a single receive antenna, which is crucial in the downlink.

Fig. 1 shows the structure used for filter adaptation. The complex-valued received signal $r_o[k] = r_{o,\mathrm{I}}[k] + j\ r_{o,\mathrm{Q}}[k]$ is prefiltered with two complex-valued filters $f_o[k] = f_{o,\mathrm{I}}[k] + j\ f_{o,\mathrm{Q}}[k]$ and $f_p[k] = f_{p,\mathrm{I}}[k] + j\ f_{p,\mathrm{Q}}[k]$. $F_o(z)$ and $F_p(z)$ denote the $z$-transforms of $f_o[k]$ and $f_p[k]$, respectively. After prefiltering, the resulting signals are projected onto $c$ and the real-valued signals $u_o[k]$ and $u_p[k]$ are obtained. The prefilters are jointly optimized with the feedback filters $b_{\nu,\mu}[k]$, where $\nu, \mu \in \{o, p\}$ and $B_{\nu,\mu}(z)$ denotes the $z$-transform of $b_{\nu,\mu}[k]$. Filters $b_{o,o}[k]$ and $b_{p,p}[k]$ must be strictly causal, whereas $b_{o,p}[k]$ and $b_{p,o}[k]$ are causal filters[1]. The training sequences of users $o$ and $p$ in the VAMOS pair are both known at the receiver of user $o$ and used for adaptation of the respective filter.

With these definitions and assumptions, the joint optimization of filters $f_o[k]$, $b_{o,o}[k]$, and $b_{o,p}[k]$ for the upper branch in Fig. 1 can be achieved by minimizing

$$\sum_{k=1}^{M} \Bigg| \sum_{\kappa=0}^{q_f} f_{o,\mathrm{I}}[\kappa] r_{o,\mathrm{I}}[k-\kappa] - \sum_{\kappa=0}^{q_f} f_{o,\mathrm{Q}}[\kappa] r_{o,\mathrm{Q}}[k-\kappa] - \sum_{\kappa=1}^{q_b} b_{o,o}[\kappa] a_o[k-k_0-\kappa] - \sum_{\kappa=0}^{q_b} b_{o,p}[\kappa] a_p[k-k_0-\kappa] - a_o[k-k_0] \Bigg|^2 \tag{16}$$

with respect to the filter coefficients, where $c = 1$ has been assumed without any loss of generality and $k_0$ is a decision delay which has to be optimized. $q_f$ and $q_b$ are the orders of the prefilter and feedback filter, respectively. For the joint optimization of filters $f_p[k]$, $b_{p,o}[k]$, and $b_{p,p}[k]$ in the lower branch, we need to minimize

$$\sum_{k=1}^{M} \Bigg| \sum_{\kappa=0}^{q_f} f_{p,\mathrm{I}}[\kappa] r_{o,\mathrm{I}}[k-\kappa] - \sum_{\kappa=0}^{q_f} f_{2,\mathrm{Q}}[\kappa] r_{o,\mathrm{Q}}[k-\kappa] - \sum_{\kappa=0}^{q_b} b_{p,o}[\kappa] a_o[k-k_0-\kappa] - \sum_{\kappa=1}^{q_b} b_{p,p}[\kappa] a_p[k-k_0-\kappa] - a_p[k-k_0] \Bigg|^2 . \tag{17}$$

Minimizing (16) and (17) is a standard least squares problem and finding the corresponding optimal filter coefficients is straightforward. After the filter adaptation, we have the following model

$$\mathbf{u}[k] = \mathbf{B}[k] * \mathbf{a}[k-k_0] + \mathbf{e}[k], \tag{18}$$

where $\mathbf{u}[k] = [u_o[k]\ u_p[k]]^T$, $\mathbf{a}[k] = [a_o[k]\ a_p[k]]^T$, $\mathbf{e}[k] = [e_o[k]\ e_p[k]]^T$ (see Fig. 1 for the definition of $e_o[k]$ and $e_p[k]$) and $\mathbf{B}[k] = \mathcal{Z}^{-1}\{\mathbf{B}(z)\}$ with

$$\mathbf{B}(z) = \begin{bmatrix} 1 + B_{o,o}(z) & B_{o,p}(z) \\ B_{p,o}(z) & 1 + B_{p,p}(z) \end{bmatrix}. \tag{19}$$

All entries of $\mathbf{B}(z)$ are causal. Thus, based on (18), a joint MIMO reduced state sequence estimation (RSSE) equalization can be performed [23].

### *E. Link-to-System Mapping*

For FER performance evaluation of the receivers a link-to-system mapping, similar to the one used in [24], is applied. The idea of the link-to-system mapping is to approximate the FER of a transmission with a mapping table, since it is too computationally complex to simulate each transmission individually. Our link-to-system mapping approach is based on two stages. In the first stage, the raw bit error rate is estimated for each burst comprising bits of a codeword representing a speech frame. This is done for each user, based on the power levels of all interferers (adjacent and co-channel), the power of the useful part of the received signal (including small-scale fading), and the SCPIR. A five-dimensional look-up table is used for this which is also dependent on the receiver algorithms since they differ in their ability to separate the users of one pair. For our simulations, we assumed that all MSs are VAMOS capable. One of the receivers described in

[1]Strictly causal means that $b_{o,o}[0] = b_{p,p}[0] = 0$ in addition to causality. Therefore, the filter output only depends on past input values, but not on the current input value.

Sections IV-A-D is employed. The look-up tables with the raw bit error rates have been generated for different values of all parameters by physical layer simulations of the respective receivers.

In the second stage, the FER is estimated based on the applied channel code and the mean value and the variance of the raw bit error rate of the bursts in the frame, cf. also [24]. Two-dimensional look-up tables were created for each GSM speech codec. This stage is independent of the algorithm used for equalization and interference cancellation. Combining these two stages efficiently models the interleaving and approximates the FER by obtaining the raw bit error rate for every burst from stage one and using the mean and variance for stage two.

## V. Radio Resource Allocation

For radio resource allocation (RRA), we assume that the BS has knowledge of the large-scale fading gain $G_i$ of each MS $i \in \mathcal{U}$ within its cell[2]. The small-scale fading and the interferer powers are unknown to the BS. For simplicity we assume that all MSs use the same speech codec[3]. In the following, RRA for the downlink case will be considered. The challenging parts of the RRA task for OSC transmission are the power allocation for the pairs and the pairing of the users.

The goal of our RRA optimization is, similar to [10], the minimization of the required sum transmit power of the BS that serves one cell. This is accomplished by finding the user pairing achieving this target. In the considered cell in total $K$ logical channels are available and $N$ users want to be served by the BS. A logical channel, in contrast to a physical channel, is not assigned to a specific frequency. There are two possibilities to use a logical channel, either by employing conventional GMSK modulation, and thereby only transmitting one user signal, or employing OSC modulation, where the logical channel is "split" into two sub-channels for two users. $\bar{K} \leq K$ channels are used for OSC transmission and therefore $\bar{N} = 2\bar{K}$ users are chosen to be paired. The $\bar{N}$ paired users are collected in the set $\mathcal{N}$. Section V-C gives details about different strategies to determine the number of channels $\bar{K}$ used for OSC transmission. The set of all possible pairs composed of the $\bar{N}$ users of set $\mathcal{N}$ is denoted by $\Pi$. There are $|\Pi| = \binom{\bar{N}}{2}$ possible pairs in set $\Pi$. The goal of the optimization is to find a pairing strategy $\mathcal{P} = \{\mathcal{P}_1, \ldots, \mathcal{P}_{\bar{K}}\}$, with $\mathcal{P}_k = \{o,\ p\}$, $\mathcal{P}_k \in \Pi$, and $k \in \{1, \ldots, \bar{K}\}$ that minimizes the total transmit power. The two users of the pair $\mathcal{P}_k$ on the $k$th logical channel are $o,\ p \in \{1, \ldots, \bar{N}\}$, where $o \neq p$. The subsets must be disjoint, i.e., $\mathcal{P}_k \cap \mathcal{P}_{k'} = \emptyset$ for $k \neq k'$.

The optimization problem can be stated as

$$\hat{\mathcal{P}} = \underset{\mathcal{P}}{\operatorname{argmin}} \sum_{i' \in \mathcal{N}} P_{i'} \tag{20}$$

under the following constraints for the users $\iota \in \{o,\ p\}$ in each pair $\mathcal{P}_k$

$$\begin{cases} P(\mathcal{P}_k) = P_o + P_p \leq P_{\max} \\ |\mathrm{SCPIR}_\iota| \leq \mathrm{SCPIR}_{\max},\ \iota \in \{o,\ p\} \\ \mathrm{FER}_\iota \leq \mathrm{FER}_{\mathrm{thr}},\ \iota \in \{o,\ p\} \end{cases}. \tag{21}$$

The first constraint limits the transmit power of each pair, $P(\mathcal{P}_k)$, to a maximum transmit power of $P_{\max}$. The absolute value of $\mathrm{SCPIR}_\iota$ is limited to $\mathrm{SCPIR}_{\max}$ for each user $\iota$ by the second constraint. The last constraint demands a frame error rate below a threshold of $\mathrm{FER}_{\mathrm{thr}}$. There are two reasons why the total transmit power is considered as a criterion. On the one hand, the interference to neighbor cells is decreased when the transmit power is lower. On the other hand, this also leads to a lower power consumption of the BS, which will help to save energy in the network operation. The optimum solution, given the assumed knowledge and the adopted criterion can be found with the algorithm proposed in Section V-B. It is possible to construct some artificial scenarios, where a feasible solution of the optimization problem cannot be found. However, for the practical scenarios considered in Section VI with moderate requirements for the FER, it was always possible to find a feasible solution to the given problem.

The main challenge is the power allocation for each user. To satisfy the FER constraint it is necessary to allocate enough power to each user to guarantee some required signal-to-interference-plus-noise ratio (SINR) at the receiver. The interference power at the receiver cannot be estimated in RRA, since the resource allocation is done independent of the other cells that use the same frequencies. Furthermore, due to frequency hopping the interference powers also change after each burst, whereas the power allocation and the pairing are fixed for at least one frame, which comprises up to 8 bursts[4]. Therefore, for RRA, it is proposed to use a simplified mapping table, compared to that proposed in Section IV-E for faster numerical evaluation. This simplified RRA mapping table will be introduced in the following.

### A. Radio Resource Allocation Mapping Table

Since the power level of the interferers is unknown to the BS, some average interference power should be assumed for RRA. Based on the mapping table described in Section IV-E a simplified RRA table is generated. As explained in Section IV-E, the link-to-system mapping table needs as input the sum powers of different interference types (adjacent channel interferers, co-channel GMSK and VAMOS interferers, etc.). The power of these different interference types is assumed to be $P_{\mathrm{int}}$ for each type. Therefore, the RRA table for interference power $P_{\mathrm{int}}$ is only a function of $\mathrm{SCPIR}_{i'}$ and $\mathrm{SNR}_{i'}$ for each user $i' \in \mathcal{N}$,

$$\mathrm{FER}_{i'} = f(\mathrm{SCPIR}_{i'}, \mathrm{SNR}_{i'}). \tag{22}$$

The table is generated for the specific number of bursts used and some assumed power delay profile for the small-scale fading such as TU.

[2]This assumption holds quite well in practice, since $G_i$ can be estimated accurately based on the received signal level (RxLev) measurements that are available at the BS.

[3]An extension to different speech codecs is straightforward.

[4]The actual number of bursts in one frame depends on the applied interleaving.

### B. Power Allocation Algorithm

The necessary transmit power for a pair can be determined by evaluating the RRA mapping table according to (22) for different values of $\mathrm{SCPIR}_i$. The $\mathrm{SCPIR}_i$ values for the evaluation are taken from the interval $[-\mathrm{SCPIR}_{\max},\ \mathrm{SCPIR}_{\max}]$. For a given pair $\mathcal{P}_k = \{o,\ p\}$, the minimum $\mathrm{SNR}_\iota$ ($\iota \in \{o,\ p\}$) necessary to fulfill the FER threshold $\mathrm{FER}_{\mathrm{thr}}$ for different values of $\mathrm{SCPIR}_\iota$ can be interpolated from the RRA mapping table. This is done by searching the smallest SNR value for the given parameters that satisfies the FER threshold and the biggest SNR value that does not satisfy the threshold. The necessary transmit power for the signal of user $\iota$, $P_\iota(\mathrm{SCPIR}_\iota)$ ($\iota \in \{o,\ p\}$), is then linearly interpolated from these entries of the mapping table for the FER threshold value. Since $\mathrm{SCPIR}_o = -\mathrm{SCPIR}_p$ and $G_o \neq G_p$, the power required for each user within the pair $\mathcal{P}_k$ will be different. The required transmit power of the VAMOS pair given the required transmit power for user $\iota$ of this pair and $\mathrm{SCPIR}_\iota$ can be calculated from

$$\tilde{P}_\iota(\mathrm{SCPIR}_\iota) = P_\iota(\mathrm{SCPIR}_\iota)/C(\mathrm{SCPIR}_\iota), \tag{23}$$

where

$$C(\mathrm{SCPIR}_\iota) = 10^{\mathrm{SCPIR}_\iota/10}/(1 + 10^{\mathrm{SCPIR}_\iota/10}) \tag{24}$$

is used to represent the individual contribution of user $\iota$ to the power of the pairing. To satisfy the FER constraint for both users the total transmit power of pairing $\mathcal{P}_k$ is selected as the maximum of the required transmit powers $\tilde{P}_\iota(\mathrm{SCPIR}_\iota)$ of both users

$$P(\mathcal{P}_k, \mathrm{SCPIR}_o) = \max(\tilde{P}_o(\mathrm{SCPIR}_o),\ \tilde{P}_p(-\mathrm{SCPIR}_o)). \tag{25}$$

The SCPIR of user $o$ is chosen as

$$\widehat{\mathrm{SCPIR}}_o = \underset{\mathrm{SCPIR}_o}{\operatorname{argmin}}\ P(\mathcal{P}_k, \mathrm{SCPIR}_o). \tag{26}$$

By that also the SCPIR chosen for user $p$, $\widehat{\mathrm{SCPIR}}_p$, is defined and the selected transmit power for pair $\mathcal{P}_k$ is

$$\hat{P}(\mathcal{P}_k) = \min(P(\mathcal{P}_k, \widehat{\mathrm{SCPIR}}_o), P_{\max}). \tag{27}$$

The $\min(\cdot)$ operation ensures that the maximum transmit power constraint is always fulfilled. However, by limiting the transmit power to $P_{\max}$, a FER higher than $\mathrm{FER}_{\mathrm{thr}}$ might result. This can be avoided by the selection of a codec with higher error correction capability.

For all possible pairs in set $\Pi$, the lowest required transmit power and the corresponding SCPIR value are calculated. The required transmit power and the respective SCPIR value are stored in matrices $\mathbf{P}$ and $\mathbf{S}$ of dimension $\bar{N} \times \bar{N}$, respectively. They are filled with $[\mathbf{P}]_{o,p} = [\mathbf{P}]_{p,o} = \hat{P}(\mathcal{P}_k)$ and $[\mathbf{S}]_{o,p} = \widehat{\mathrm{SCPIR}}_o$ and $[\mathbf{S}]_{p,o} = -\widehat{\mathrm{SCPIR}}_o$, respectively. Since our optimization problem is a weighted perfect matching problem in non-bipartite graphs [25], the *Blossom Algorithm* can be applied on the transmit power matrix $\mathbf{P}$ to find the pairing with the lowest sum power. The algorithm finally returns the pairing $\hat{\mathcal{P}}$ that fulfills (20) under the constraints in (21). The values for the transmit powers of the users and the SCPIR can be extracted from $\mathbf{P}$ and $\mathbf{S}$, respectively. The powers of users $o$ and $p$ of the $k$th pair can be computed as $P_o = [\mathbf{P}]_{o,p} \cdot C([\mathbf{S}]_{o,p})$ and $P_p = [\mathbf{P}]_{p,o} \cdot C([\mathbf{S}]_{p,o})$, respectively.

The power allocation for a single user with GMSK modulation is straightforward. With an RRA mapping table for the FER that only depends on the SNR of the user, the necessary transmit power can be easily assigned.

### C. User Pairing Strategies

There are different possible strategies to decide which users should be paired and which should transmit alone. The number of logical channels $\bar{K}$ that are used for OSC transmission must be determined by some pairing strategy. As a reference, the *no-VAMOS* case is of interest where $\bar{K} = 0$ logical channels use OSC transmission. Therefore, only up to $K$ randomly selected users can be served with GMSK modulation. If $N > K$, the remaining users will be blocked and cannot be served. To see the effect of *pure VAMOS*, where as many users as possible are paired, $\bar{K} = \min(K, \lfloor N/2 \rfloor)$ OSC transmissions are used. If $N < 2K$ and $N$ odd, one randomly selected user transmits without VAMOS. If $N > 2K$, $N - 2K$ users are blocked. For the case of $N < 2K$ some channels may remain unused, since there are more logical channels than pairs.

Another option is to only pair users if $N > K$. The *pair only if otherwise blocked* (POOB) strategy will be identical to the no-VAMOS case if $N \leq K$ and is identical to pure VAMOS if $N \geq 2K$. For $K < N < 2K$, $\bar{K} = N - K$ channels are used for OSC transmission and $K - \bar{K}$ channels are used with GMSK modulation. For all strategies, the users that are served with OSC or GMSK transmission are chosen at random.

To reduce the complexity of the RRA, it is also possible to use a random pairing instead of optimizing the pairing according to (20) and (21), for which $|\Pi|$ possible pairs have to be evaluated. For the optimization of SCPIR, one can set $\mathrm{SCPIR}_i = 0$ dB $\forall i \in \{1,\ \ldots,\ N\}$, which corresponds to equal user powers within one pair. Another possibility is to combine random pairing with SCPIR optimization for each of the randomly formed pairs. The computational complexity is much lower than for optimum user pairing, since only for $\bar{K}$ pairs the optimum SCPIR must be determined according to (26).

## VI. Simulation Results

This section presents simulation results for channel estimation, receiver algorithms and network simulations.

### A. Channel Estimation and Receiver Algorithms

In the following, simulation results for channel estimation and an evaluation of the performance of different receiver algorithms are presented. In Fig. 2, the sum mean-squared error (MSE)[5] for VAMOS channel estimation is compared with the Cramer-Rao Lower Bound (CRB) for conventional GMSK transmission [26] and the CRB for VAMOS, derived in [8]. The joint ML estimation from Section III-A is applied for VAMOS channel estimation. The SCPIR value is set to

[5] The sum MSE is defined as the sum of the MSEs of the estimates of the individual channel taps.

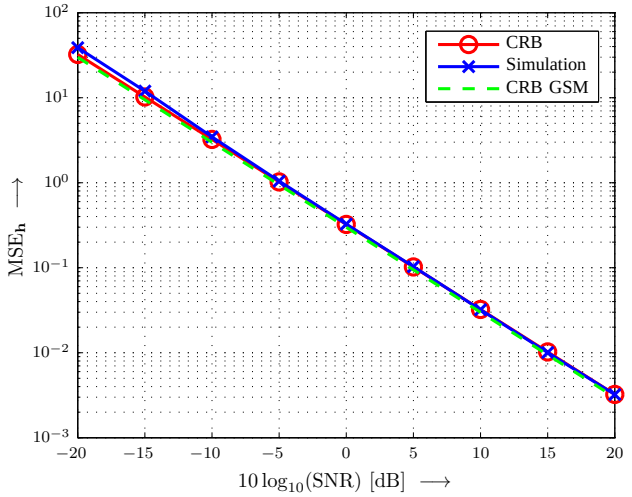


Fig. 2. Sum MSE versus SNR for the estimation of the channel coefficients ($b = 1$).

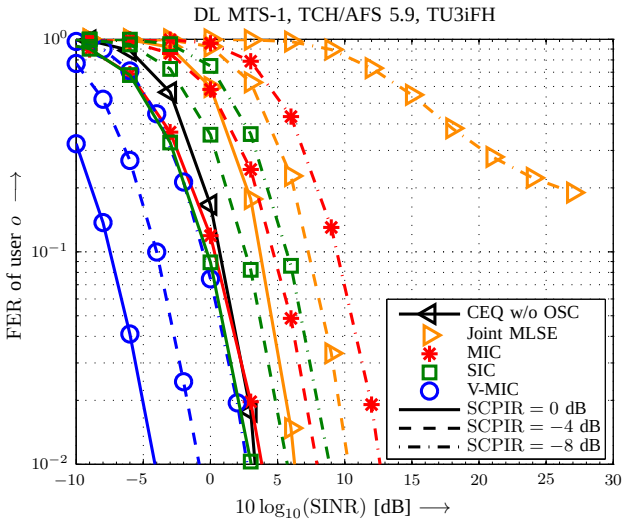


Fig. 3. FER of user $o$ versus SINR for MTS-1 scenario and different receivers.

TABLE I
MTS-1 AND MTS-2 INTERFERENCE SCENARIOS [7].

| Scenario | Interfering signal | Interferer relative power |
|---|---|---|
| MTS-1 | Co-channel 1 | 0 dB |
| MTS-2 | Co-channel 1 | 0 dB |
| | Co-channel 2 | −10 dB |
| | Adjacent channel 1 | 3 dB |
| | AWGN | −17 dB |

$b = 1$, while 5000 different channel impulse responses of order $q_h = 5$ have been generated with independent taps drawn from a random complex normal distribution with zero mean and variance $\sigma_h^2 = 1/(q_h + 1)$. The SNR of user $o$ relevant for channel estimation for OSC transmission is $\mathrm{SNR}^{\mathrm{OSC}} = (1 + b^2)\sigma_a^2/\sigma_{n_o}^2$, while for conventional GSM transmission the relevant SNR is $\mathrm{SNR}^{\mathrm{GMSK}} = \sigma_a^2/\sigma_{n_o}^2$, to ensure a fair comparison. For OSC transmission, we can exploit the power of both subchannels since both training sequences are known. However, for non-OSC transmission, only the transmit power of the user of interest can be used since all interferers have unknown training sequences. Training sequence code (TSC) 0 and the corresponding VAMOS TSC 0 [7] have been used for the simulations.

The proposed estimator matches the CRB closely for a broad range of SNR values. Only for low SNRs a minor degradation is visible. A loss in channel estimation accuracy compared to channel estimation for conventional GSM transmission is barely visible for the considered SCPIR value of 0 dB. In [8] also results for the estimation of the SCPIR can be found which show a similarly good MSE performance.

For evaluation of the different receiver algorithms, a TU channel profile is considered for an MS speed of 3 km/h (TU3). Ideal frequency hopping over $N_{\mathrm{bursts}} = 8$ bursts is used in the 900 MHz band. Again, TSC 0 and VAMOS TSC 0 have been used. Speech transmission with adaptive multirate (AMR) speech coding with full rate (TCH/AFS 5.9 codec) is investigated. It is shown in [27] that mean opinion score (MOS) gains for speech quality can be achieved by using full rate speech coding in conjunction with OSC instead of half rate speech coding with non-OSC transmission. For the interference from other cells, the MTS-1 and MTS-2 models from [7] have been used. In MTS-1, only a single co-channel interferer is present, while MTS-2 defines an interference mixture. The details are given in Table I. All interferers use GMSK modulation, and their TSCs are randomly chosen from the eight specified GMSK TSCs. The interferers are synchronized with the desired signal.

In the receiver, channel estimation and filter adaptation were used and a time slot based frequency offset compensation was active. Receiver impairments such as phase noise and I/Q imbalance were taken into account, and typical values for an implementation were selected, cf. [21].

In Fig. 3, the FER of user $o$ after channel decoding versus SINR is shown for joint MLSE, MIC, SIC, and V-MIC for the MTS-1 scenario. In general, SINR denotes the power of the OSC signal of both users, received by MS $o$, divided by the power of co-channel interferer 1 according to Table I. Results for different SCPIR values are shown. Also depicted is the performance of the conventional GSM equalizer (CEQ) without interference suppression capabilities for a pure GMSK transmission. For an SCPIR value of 0 dB MIC and SIC perform very similar, but the V-MIC shows a significant improvement of about 8 dB in SINR for the same FER. A very similar gain of V-MIC compared to MIC and SIC can also be observed for lower SCPIR values. One can conclude from Fig. 3 that it is possible to cancel one interferer quite well with the advanced V-MIC structure, while the degradation of the other receivers is more significant for low SCPIR values. The joint MLSE receiver is beneficial for noise limited scenarios, cf. [12], but for interference limited scenarios this receiver has a very poor FER performance. This can be explained by the fact that the joint MLSE cannot mitigate interference but treats it as noise. Therefore, a severe performance degradation

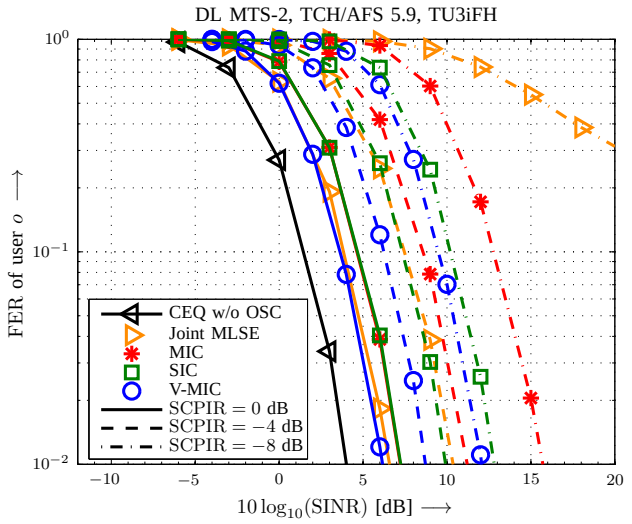


Fig. 4. FER of user $o$ versus SINR for MTS-2 scenario and different receivers.

occurs in particular for low SCPIR values.

For the MTS-2 scenario considered in Fig. 4, not only one GMSK interferer is present but multiple interferers, cf. Table I. The novel V-MIC achieves a gain of 1 dB compared to the SIC and MIC receivers for an SCPIR of 0 dB and the FER is also better than that for joint MLSE. The lower gain of V-MIC compared to the MTS-1 scenario is due to the higher number of interferers. Such an interference mixture cannot be combated as well as a single interferer. The loss of MIC compared to SIC and V-MIC, respectively, increases for lower SCPIR values, while the gain of V-MIC is still 1 dB compared to SIC. The performance of joint MLSE degrades severely for lower SCPIR values which has been also observed for MTS-1.

### *B. Network Simulations*

Table II gives an overview of the parameters used for the simulation results for RRA. Only one of the 8 periodic GSM time slots has been simulated. Ideal random frequency hopping over all available frequencies in each cell is used. In contrast to Section VI-A, here the AMR half rate speech codec with a bit rate of 5.9 kbps (AHS 5.9) is used for all simulations to maximize the network capacity. All cells are frame synchronized and $\text{FER}_{\text{thr}} = 1\%$. The power of each interference type relative to the noise power $P_{\text{int}}$ is used for RRA since the true interference power is not known. For the network performance evaluation, the true interference power is calculated according to the distribution of all users in all cells. All interferers can be either OSC or GMSK modulated, depending on the decisions made by the RRA algorithm.

The network simulator first generates new cells and then randomly distributes users in the cells. On a cell per cell basis one of the RRA algorithms from Section V is executed. The logical channels are then randomly assigned to the physical channels. For all users in all cells, realizations of the small-scale fading are generated for each of the 4 bursts involved in a frame, and the FER is evaluated according to Section IV-E. Then, all users are removed from the cells and the procedure

TABLE II
SIMULATION PARAMETERS.

| | |
|---|---|
| cell radius [m] | 500 |
| sectors per cell | 1 |
| reuse factor | 12 |
| number of clusters | 9 |
| small-scale fading | Typical Urban (TU) |
| pathloss model | UMTS 30.03, Vehicular Test Env. |
| distance attenuation coefficient | 3.76 |
| gain at 1 m distance [dB] | −8.06 |
| standard deviation for the log-normal fading [dB] | 8 |
| channels available in each cell | $K = 8$ |
| max. transmit power [dBm] | $P_{\max} = 30$ |
| noise power [dBm] (thermal noise + noise figure) | $-119.65 + 8$ |
| $\text{SCPIR}_{\max}$ [dB] | 12 |
| number of bursts for frequency hopping | $N_{\text{bursts}} = 4$ |
| power of each interference type relative to noise power [dB] | $P_{\text{int}} = \{10, 13, 15\}$ |
| speech codec | AHS 5.9 (half rate) |
| carrier frequency [MHz] | 900 |

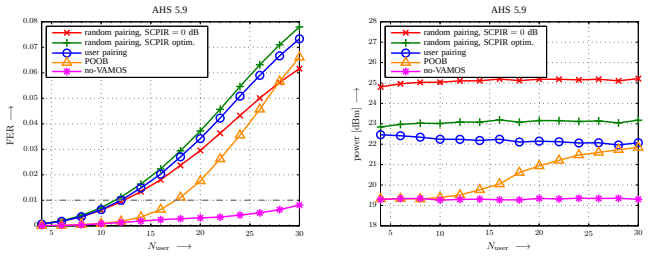


(a) FER. (b) Average transmit power of BS per MS.

Fig. 5. FER and transmit power vs. average number of users per cell for VAMOS vs. no-VAMOS scenario, $P_{\text{int}} = 10$ dB above noise power, MIC receiver.

starts from the beginning with the random distribution of new users in the cells, i.e., there is no simulation over time. The total number of users in all cells is fixed and the users are randomly dropped into the total area which results in an average number of users per cell $N_{\text{user}}$.

Figs. 5(a) and 5(b) depict the FER and the average transmit power of the BS per MS over the average number of users per cell $N_{\text{user}}$, respectively. A MIC receiver was used at all MSs. The lines marked with "random pairing, SCPIR = 0 dB" show the performance of random user pairing and equal power allocation within each pair ($\text{SCPIR} = 0$ dB). Fig. 5(b) shows that by optimizing the SCPIR for all random pairs ("SCPIR optim."), a power reduction of nearly 2 dB is possible. The additional power saving enabled by employing optimal user pairing ("user pairing") compared to random user pairing and SCPIR optimization is about 0.5 dB, and increases with the number of users available for user pairing. For these three cases all users were forced to always transmit over OSC

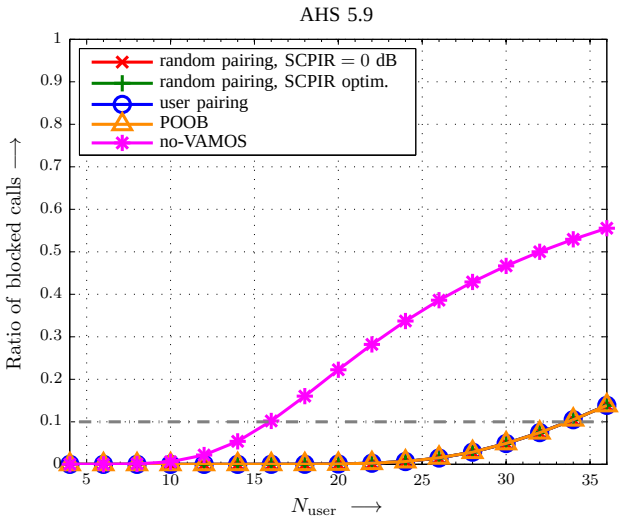


Fig. 6. Ratio of blocked calls versus average number of users per cell for VAMOS vs. no-VAMOS scenario, $P_{\text{int}} = 10$ dB above noise power, MIC receiver.

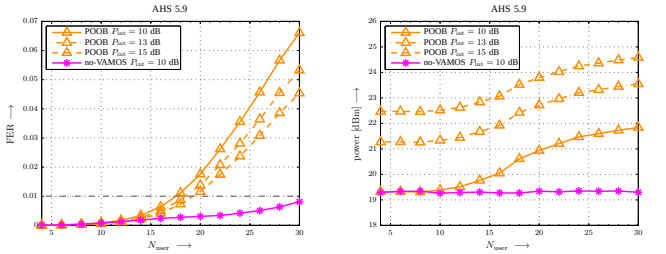


(a) FER. (b) Average transmit power of BS per MS.

Fig. 7. FER and transmit power versus average number of users per cell for different $P_{\text{int}}$ values, MIC receiver.

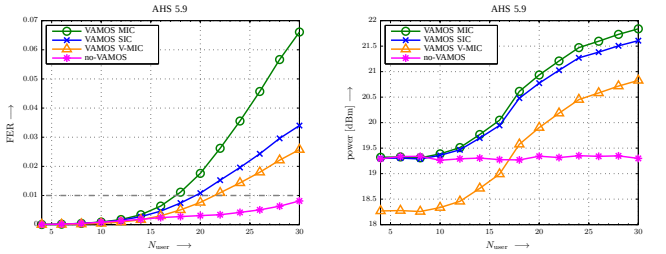


(a) FER. (b) Average transmit power of BS per MS.

Fig. 8. FER and transmit power versus average number of users per cell for different receivers, $P_{\text{int}} = 10$ dB above noise power, POOB user pairing.

channels. One can see that the power required for transmission is about 3 dB higher than for transmission without VAMOS. This is due to the fact that the power allocation for a single user only needs to achieve the SNR target for that user, not for both users, cf. (25). When only pairing users that would be blocked if no OSC was used ("POOB"), one can see that the necessary power lies between no-VAMOS and VAMOS with user pairing. For a low average number of users in the cell, e.g. between $N_{\text{user}} = 4$ and 8, the necessary power is equal to that of the no-VAMOS case. By increasing $N_{\text{user}}$, the number of users that receive their signal via OSC transmission increases and thereby also the necessary transmit power.

The FER of the different pairing strategies is depicted in Fig. 5(a). One can see that an $\text{FER}_{\text{thr}}$ (dash dotted line) of 1 % cannot be fulfilled for a high number of users in the cell and OSC transmission. When the load in the cells increases, also the co-channel interference increases dramatically. The MIC receiver that is employed for all cases cannot cancel all interferers anymore which leads to an increased FER. Even for the no-VAMOS case, where also the MIC receiver is used, the FER approaches the threshold for a high number of users. For the user pairing algorithms that try to pair as many users as possible the interference is very often an OSC signal that cannot be cancelled by the MIC receiver. This can also be seen for the MTS-2 scenario investigated in Fig. 4. For the cases with high load, the FER performance of user pairing is worse than without user pairing. The resource allocation has been optimized for a fixed value of interference power $P_{\text{int}}$. Different values for $P_{\text{int}}$ will be considered in Fig. 7. However, the actual interference power caused by the different algorithms exceeds this value already for a medium system load. One can also observe that the lower transmit power that is achieved by user pairing compared to random pairing, results in a worse FER for high load.

From Fig. 5 one could come to the conclusion that no-VAMOS would be the better choice. However, when taking into account the number of blocked calls, depicted in Fig. 6, the main benefit of VAMOS is revealed. Here, we assume a call is blocked if not enough logical channels are available to schedule this call. For our simulations, $K = 8$ physical channels are available per cell. Compared to full rate, with the half rate codec the number of available logical channels per cell is doubled. As one can see from Fig. 6, the percentage of blocked calls increases very fast for the no-VAMOS case. Already for $N_{\text{user}} = 16$ the percentage of blocked calls exceeds 10 % (dash dotted line). In contrast, by employing the OSC concept, 10 % blocked calls occur for $N_{\text{user}} = 33.7$. The average number of users for a given percentage of blocked calls can be more than doubled by doubling the number of available channels with VAMOS. This can be explained with the Erlang B formula for the blocking probability, which states that by increasing the number of available channels the blocking probability decreases for the same relative load. This capacity gain is the reason why the OSC concept was introduced in GSM.

A solution to overcome the undesirable FER behavior observed in Fig. 5 is to increase $P_{\text{int}}$ for RRA, which will result in a higher power consumption. Figs. 7(a) and 7(b) show the FER and transmit power, respectively, for different values of $P_{\text{int}}$. It can be seen that by increasing the assumed interference power also the transmit power is increased which has a positive influence on the FER performance. Still, for a load higher than 19 users, the FER threshold cannot be satisfied anymore for a VAMOS transmission.

Therefore, the key to avoid the undesirable FER behavior without increasing $P_{\text{int}}$ is to use an enhanced receiver in the MSs. Figs. 8(a) and 8(b) show the FER and transmit power,

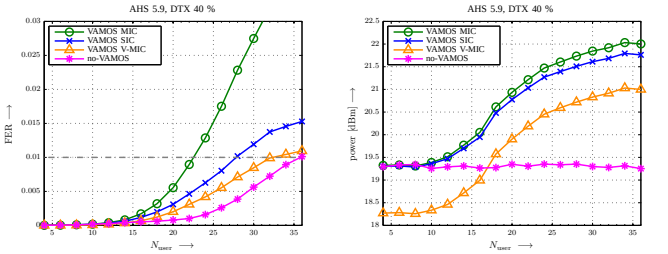


(a) FER. (b) Average transmit power of BS per MS.

Fig. 9. FER and transmit power versus average number of users per cell for different VAMOS receivers, $P_{\text{int}} = 10$ dB above noise power, DTX enabled, POOB user pairing.

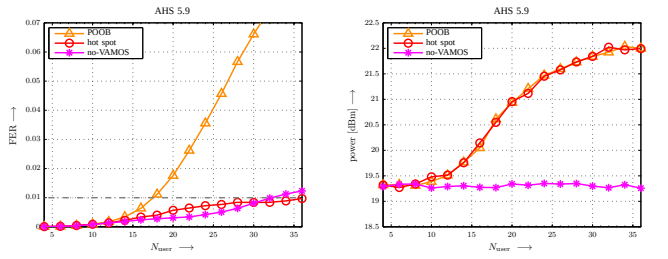


(a) FER. (b) Average transmit power of BS per MS.

Fig. 10. FER and transmit power versus average number of users per cell, MIC receiver, hot spot scenario, $P_{\text{int}} = 10$ dB above noise power.

respectively, for POOB user pairing if MIC, SIC, and V-MIC receivers are employed at the MSs, respectively. Due to the better interference cancellation capabilities of the SIC and V-MIC receivers, the FER is much lower than for the MIC receiver. For the SIC receiver a small transmit power saving compared to MIC can be achieved, whereas for V-MIC the RRA can reduce the transmit power significantly.

The FER and transmit power, respectively, for a more realistic scenario with enabled discontinuous transmission (DTX), where a scheduled user does not transmit due to no speech activity with a probability of 40%, are depicted in Figs. 9(a) and 9(b). The POOB pairing strategy has been used for the VAMOS results. The interference situation is now more relaxed compared to the case without DTX. Within one pair, only with a probability of 36% both users are active, while both users of one pair are silent with a probability of 16%. This means that strong interference by OSC users does not occur very often. Furthermore, when the second user is not present, the receiver can use its interference rejection capabilities to better suppress co-channel interferers from other cells. With the V-MIC receiver it is now possible to keep the FER below 1% for $N_{\text{user}} \leq 32$. This enables a very high user load in the system.

In Figs. 10(a) and 10(b), the FER and transmit power, respectively, for a hot spot scenario are depicted. A comparison is made with a no-VAMOS GMSK modulated transmission and OSC transmission with POOB user pairing in all cells. DTX is deactivated in all cases and a MIC receiver is employed in all MSs. For the hot spot scenario the cell layout is not changed compared to the scenarios in Figs. 5-9. However, for the hot spot scenario only one cell (the hot spot) uses OSC transmission and all other co-channel cells use legacy GSM with GMSK modulation. Only the FER of the hot spot cell is shown here. One can also view this scenario as perfect frequency assignment, where all co-channel cells schedule the OSC users in such a way that only GMSK interferers are present for an OSC pair. It can be observed that the resulting FER for the hot spot scenario is always below 1%. This shows that the FER reduction due to the missing OSC interference is significant. However, this also suggests that in other work, such as [10], where only GMSK interference is assumed, the actually achievable performance of a fully loaded VAMOS network may be overestimated. We note that especially for the case of a high load in all cells, perfect frequency assignment over all cells guaranteeing only GMSK interference for the OSC users is impossible. To have a fair performance comparison of the hot spot scenario with POOB, we use for the hot spot scenario the same transmit power allocation that is also used in the case of OSC interference for all cells. For $N_{\text{user}} > 30$, the FER of the hot spot is even lower than that of the no-VAMOS scenario with GMSK modulation. This is a consequence of the higher transmit power allocation in the hot spot scenario compared to the no-VAMOS scenario.

TABLE III
OVERALL NETWORK CAPACITY GAIN OF OSC COMPARED TO NON-OSC TRANSMISSION WITH $P_{\text{int}} = 10$ dB.

| Scenario | OSC gain |
|---|---|
| POOB, MIC, no DTX | 9.4% |
| POOB, SIC, no DTX | 21.9% |
| POOB, V-MIC, no DTX | 34.4% |
| POOB, MIC, DTX | 40.6% |
| POOB, SIC, DTX | 75.0% |
| POOB, V-MIC, DTX | 103% |
| hot spot, MIC, no DTX | 112% |

Table III summarizes the overall network capacity gain of OSC transmission for different parameters compared to no-VAMOS transmission with the MIC receiver, where $P_{\text{int}} = 10$ dB is valid for all cases. The gain is computed by comparing the maximum number of users with FER $< 1\%$ and blocked calls $< 10\%$ for each case. As a reference we use the no-VAMOS transmission, where 10% blocked calls occur for $N_{\text{user}} = 16$. In all considered cases, a network capacity gain of OSC compared to no-VAMOS can be observed. With DTX enabled, the new V-MIC exhibits a network capacity gain of more than 100%. For the hot spot with a MIC receiver, when OSC is only used in one cell, even more than 100% network capacity gain can be achieved.

## VII. CONCLUSIONS

In this paper, different receiver concepts for OSC downlink transmission used in VAMOS have been introduced. Channel estimation algorithms have been proposed, and different receivers for OSC transmission over frequency-selective fading channels with interference have been introduced and compared with respect to their frame error rate performance. It was shown that the novel V-MIC receiver exhibits a significant

performance improvement compared to receivers from the literature. A practical transmit power allocation and user pairing algorithm has been proposed as well. Different receiver concepts have been evaluated in a network scenario using the proposed radio resource allocation algorithm. The benefits of discontinuous transmission and the strong dependence of the VAMOS downlink performance on the type of interference have been shown. Capacity gains of more than 100% compared to no-VAMOS transmission can be obtained with the novel V-MIC receiver in a realistic network scenario.

In summary, powerful solutions for the reception of OSC downlink signals have been developed in this paper. These receivers combined with the proposed radio resource allocation schemes achieve a very good performance even if exact knowledge of the interference situation is not available for resource allocation.

## REFERENCES


[1] R. Meyer, W. Gerstacker, R. Schober, and J. B. Huber, "A Single Antenna Interference Cancellation Algorithm for Increased GSM Capacity," *IEEE Transactions on Wireless Communications*, vol. 5, no. 7, pp. 1616–1621, 2006.

[2] P. Chevalier and F. Pipon, "New Insights Into Optimal Widely Linear Array Receivers for the Demodulation of BPSK, MSK, and GMSK Signals Corrupted by Noncircular Interferences - Application to SAIC," *IEEE Transactions on Signal Processing*, vol. 54, pp. 870–883, 2006.

[3] Nokia, *3GPP Tdoc GP-071792, Voice Capacity Evolution with Orthogonal Sub Channels*, 3GPP TSG GERAN #36, Vancouver, Canada, Nov. 2007.

[4] X. Chen, Z. Fei, J. Kuang, L. Liu, and G. Yang, "A Scheme of Multi-user Reusing One Slot on Enhancing Capacity of GSM/EDGE Networks," in *Proc. of 11th IEEE Singapore International Conference on Communication Systems (ICCS 2008)*, Singapore, Nov. 2008, pp. 1574–1578.

[5] M. Säily, J. Hulkkonen, K. Pedersen, C. Juncker, R. Paiva, R. Iida, O. Piirainen, S. Sundaralingam, A. Loureiro, J. Helt-Hansen, R. Domingos, and F. Tavares, *GSM/EDGE: Evolution and Performance*. John Wiley & Sons, 2011, ch. Orthogonal Sub-Channels with AMR/DARP, pp. 235 – 276.

[6] R. C. D. Paiva, R. D. Vieira, R. Iida, F. M. Tavares, M. Saily, J. Hulkkonen, R. Jarvela, and K. Niemela, "GSM Voice Evolution Using Orthogonal Subchannels," *IEEE Communications Magazine*, vol. 50, no. 12, pp. 80–86, 2012.

[7] *3GPP TR 45.914, Circuit switched voice capacity evolution for GSM/EDGE Radio Access Network (GERAN), version 9.4.0*, Nov. 2010.

[8] M. A. Ruder, R. Schober, and W. H. Gerstacker, "Cramer-Rao Lower Bound for Channel Estimation in a MUROS/VAMOS Downlink Transmission," in *Proc. IEEE 22nd Int. Personal Indoor and Mobile Radio Communications (PIMRC) Symp.*, 2011, pp. 1433–1437.

[9] M. G. Vutukuri, R. Malladi, K. Kuchi, and R. D. Koilpillai, "SAIC Receiver Algorithms for VAMOS Downlink Transmission," in *Proc. 8th Int. Wireless Communication Systems (ISWCS) Symp.*, 2011, pp. 31–35.

[10] D. Molteni, M. Nicoli, and M. Säily, "Resource Allocation Algorithm for GSM-OSC Cellular Systems," in *Proc. IEEE Int. Conf. on Communications (ICC)*, 2011, pp. 1–6.

[11] M. A. Ruder, R. Meyer, H. Kalveram, and W. H. Gerstacker, "Radio Resource Allocation for OSC Downlink Channels," in *Proc. of 1st IEEE Int. Conf. on Communications in China (ICCC), Workshop on Smart and Green Communications & Networks (SGCNet)*, 2012, pp. 113–118.

[12] R. Meyer, W. H. Gerstacker, F. Obernosterer, M. A. Ruder, and R. Schober, "Efficient Receivers for GSM MUROS Downlink Transmission," in *Proc. IEEE 20th Int. Personal, Indoor and Mobile Radio Communications Symp. (PIMRC)*, 2009, pp. 2399–2403.

[13] *3GPP TS 45.004, Modulation, version 11.0.0*, Sep. 2012.

[14] S. Crozier, D. Falconer, and S. Mahmoud, "Least Sum of Squared Errors (LSSE) Channel Estimation," *IEE Proceedings F*, vol. 138, pp. 371–378, Aug. 1991.

[15] R. P. Brent, *Algorithms for Minimization without Derivatives*. Englewood Cliffs, New Jersey: Prentice-Hall, 1973.

[16] M. Fossorier, F. Burkert, S. Lin, and J. Hagenauer, "On the Equivalence between SOVA and Max-Log-MAP Decodings," *IEEE Communications Letters*, vol. 2, no. 5, pp. 137–139, May 1998.

[17] W. Koch and A. Baier, "Combined Design of Equalizer and Channel Decoder for Digital Mobile Radio Receivers," *Proceedings of ITG Conference „Stochastische Modelle und Methoden in der Informationstechnik"*, pp. 263–270, Apr. 1989.

[18] *3GPP TS 45.005, Radio Transmission and Reception (Release 9), version 9.13.0*, Mar. 2013.

[19] R. Meyer, W. Gerstacker, and R. Schober, "Method for Cancelling Interference during TDMA Transmission and/or FDMA Transmission," Patent, Dec., 2000.

[20] R. Meyer, W. Gerstacker, R. Schober, and J. B. Huber, "A Single Antenna Interference Cancellation Algorithm for GSM," in *Proc. of Vehicular Technology Conf. (VTC 2005-Spring)*, Stockholm, Sweden, May / June 2005.

[21] Com-Research, *3GPP Tdoc GP-100083, VAMOS Downlink Receiver Performance for CCI and ACI Scenarios*, 3GPP TSG GERAN #45, Berlin, Germany, Mar. 2010.

[22] D. Molteni and M. Nicoli, "A Novel Uplink Receiver for GSM/EDGE Systems with Orthogonal Sub Channel Feature," in *Proc. of the Forty-Third Asilomar Conf. on Signals, Systems, and Computers*, 2009, pp. 977–981.

[23] J. Zhang, A. Sayeed, and B. Van Veen, "Reduced-state MIMO Sequence Detection with Application to EDGE Systems," *IEEE Transactions on Wireless Communications*, vol. 4, no. 3, pp. 1040–1049, May 2005.

[24] S. Brueck, H.-J. Kettschau, and F. Obernosterer, "Emission Reduction and Capacity Increase in GSM Networks by Single Antenna Interference Cancellation," *AEU - International Journal of Electronics and Communications*, vol. 58, no. 4, pp. 274–283, 2004.

[25] C. Papadimitriou and K. Steiglitz, *Combinatorial Optimization: Algorithms and Complexity*. Dover Publications, 1998.

[26] E. De Carvalho and D. T. M. Slock, "Cramer-Rao Bounds for Semi-blind, Blind and Training Sequence based Channel Estimation," in *Proc. First IEEE Signal Processing Workshop Signal Processing Advances in Wireless Communications*, 1997, pp. 129–132.

[27] R. C. D. Paiva, R. Vieira, R. Järvelä, R. Iida, F. Tavares, and M. Säily, "Improving the Speech Quality with OSC: Double Full-Rate Performance Assessment," in *Proc. IEEE 72nd Vehicular Technology Conf. Fall (VTC 2010-Fall)*, 2010, pp. 1–5.